

## LETTERS

# Unique features of action potential initiation in cortical neurons

Björn Naundorf<sup>1,2,3</sup>, Fred Wolf<sup>1,2,3</sup> & Maxim Volgushev<sup>4,5</sup>

Neurons process and encode information by generating sequences of action potentials<sup>1,2</sup>. For all spiking neurons, the encoding of single-neuron computations into sequences of spikes is biophysically determined by the cell's action-potential-generating mechanism. It has recently been discovered that apparently minor modifications of this mechanism can qualitatively change the nature of neuronal encoding<sup>3,4</sup>. Here we quantitatively analyse the dynamics of action potential initiation in cortical neurons *in vivo*, *in vitro* and in computational models. Unexpectedly, key features of the initiation dynamics of cortical neuron action potentials—their rapid initiation and variable onset potential—are outside the range of behaviours described by the classical Hodgkin–Huxley theory. We propose a new model based on the cooperative activation of sodium channels that reproduces the observed dynamics of action potential initiation. This new model predicts that Hodgkin–Huxley-type dynamics of action potential initiation can be induced by artificially decreasing the effective density of sodium channels. *In vitro* experiments confirm this prediction, supporting the hypothesis that cooperative sodium channel activation underlies the dynamics of action potential initiation in cortical neurons.

We analysed action potentials elicited in cortical neurons *in vivo* and *in vitro*, either spontaneously or in response to various stimuli. In all cells examined and for all conditions tested, the dynamics of action potential initiation was characterized by a very abrupt onset and a steep upstroke in membrane potential. In membrane potential traces, the abrupt onset of action potentials is apparent as a sharp kink (Fig. 1a, c). This phenomenon stands out even more clearly in phase plots that graph the rate of change of the membrane potential  $dV/dt$  against the instantaneous membrane potential  $V(t)$ , and is manifested as an almost vertical take-off in  $dV/dt$  versus  $V$  trajectories at action potential onset (Fig. 1b, d). In phase plots, an action potential is represented by a loop. At the start of the loop, the velocity increases rapidly from less than  $5 \text{ mV ms}^{-1}$  to more than  $20 \text{ mV ms}^{-1}$ . This several-fold increase in velocity occurs within a range of less than 1 mV and takes less than 0.2 ms. This onset behaviour is not a peculiarity of neurons *in vivo*. Neurons *in vitro* show similarly fast dynamics of action potential initiation (Fig. 1c, d). These dynamic features of recorded action potential onsets distinguish them from the behaviour of previously proposed computational models. Figure 1e, f shows a simulated action potential using a recently developed conductance-based model of a cortical neuron<sup>5</sup>. In this model, a velocity of  $20 \text{ mV ms}^{-1}$  is only reached over a range of 7–8 mV after about 1 ms. Thus, the real onset of cortical action potentials is approximately ten times faster than predicted by the model.

The rapid onset of action potentials is a very robust phenomenon, apparent during spontaneous and evoked activity *in vivo*. Moreover,

it is independent of the temporal structure of synaptic inputs (Fig. 2) and of the electrophysiological cell class (Fig. 4). Fig. 2 shows phase plots and membrane potential traces from a simple cell (Fig. 2a, b) and a complex cell (Fig. 2c, d) recorded *in vivo* in cat visual cortex. In the phase plots, subthreshold membrane potential fluctuations are represented by a grey cloud. In both the simple and the complex cell, action potentials rise almost vertically out of this cloud. Detecting the point at which the rate of change reaches a value of  $10 \text{ mV ms}^{-1}$  thus allows reliable identification of the time of action potential initiation

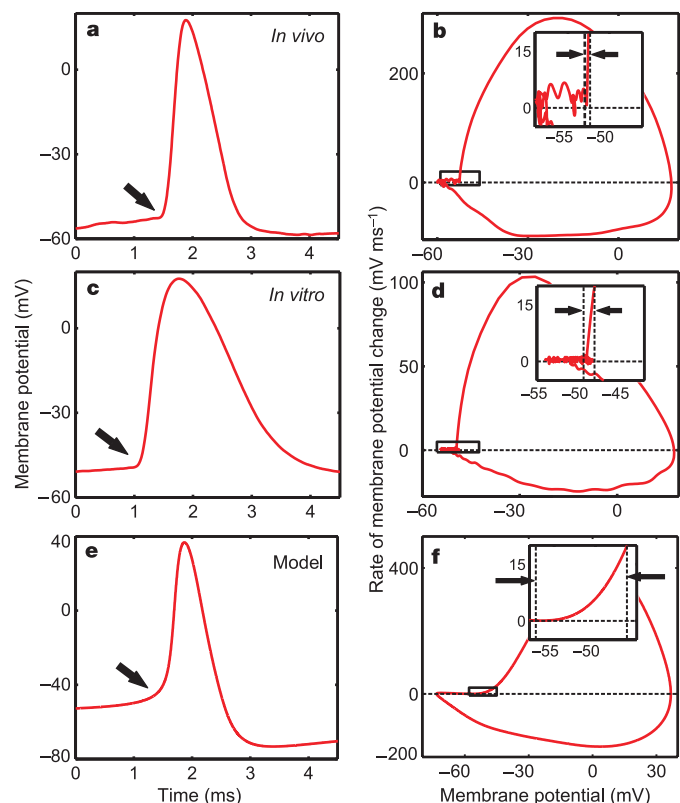


**Figure 1 | Dynamics of action potential initiation in neocortical neurons and in a Hodgkin–Huxley-type model of a neocortical neuron.** **a**, Action potential in a cat visual cortex neuron *in vivo*. The arrow shows the characteristic kink at action potential onset. **b**, Phase plot ( $dV/dt$  versus  $V$ ) of the action potential from **a**. Inset shows the initial phase of the action potential. **c**, **d**, Action potential from a cat visual cortical slice *in vitro* at  $20^\circ\text{C}$ . **e**, **f**, Action potential from a Hodgkin–Huxley-type model of a neocortical neuron<sup>5</sup>.

<sup>1</sup>Max Planck Institute for Dynamics and Self-Organization, <sup>2</sup>Department of Physics and <sup>3</sup>Bernstein Center for Computational Neuroscience, University of Göttingen, Bunsenstr. 10, D-37073 Göttingen, Germany. <sup>4</sup>Department of Neurophysiology, Ruhr-University Bochum, D-44780 Bochum, Germany. <sup>5</sup>Institute of Higher Nervous Activity and Neurophysiology Russian Academy of Sciences, Moscow 117485, Russia.

and the onset potential. The phase plots also show a second salient feature of cortical action potentials: the onset potentials vary considerably, over ranges of up to 10 mV (Fig. 2a–d) (Special care was taken to exclude any non-stationarities, see Supplementary Information). This distinct variability in onset potentials has previously been observed in cat visual cortex<sup>6–8</sup> and rat hippocampus<sup>9</sup>. This second feature of cortical action potentials is also missing in Hodgkin–Huxley-type models. Figure 2e, f depicts the behaviour of such a model driven by fluctuating synaptic inputs<sup>5</sup>. The variability in onset potentials in this model is restricted to a range of less than 2 mV, which is much smaller than observed *in vivo*.

Two features thus render cortical action potentials distinctly different from simulated action potentials using Hodgkin–Huxley-type models. First, the initial action potential phase is approximately ten times faster in recorded neurons compared to conductance-based models. Second, the onset potential variability is approximately five times larger in the recorded cells. We tried, using various modifications of the models, to achieve a better match between recorded and simulated action potentials (including and/or modifying adaptation currents<sup>10</sup>, channel stochasticity<sup>11</sup>, state-dependent inactivation<sup>12</sup>, sodium channel activation curves and peak conductances; see Supplementary Information). None of the modified models reproduced the two salient features of the recorded action potentials.

In fact, a straightforward analysis reveals that rapid action potential onset and large variability in onset potentials are strongly antagonistic in Hodgkin–Huxley-type models. In such models, the initial phase of an action potential is determined by the activation of

voltage-dependent sodium channels. Their dynamics is described by the activation curve and kinetics of an associated gating variable. In the Hodgkin–Huxley formulation it can be shown that the rate of membrane depolarization is limited by  $g_{\text{Na}}h_0m_{\infty}^3(V)(V_{\text{Na}} - V)/C + I_0/C$ , where  $g_{\text{Na}}$  denotes peak sodium conductance,  $h_0$  is the fraction of sodium channels available for activation,  $m_{\infty}^3(V)$  is their activation curve,  $V_{\text{Na}}$  is the sodium reversal potential,  $C$  the membrane capacitance, and  $I_0$  is the current carried by other channels. This upper bound on the rate of membrane potential change links the action potential onset dynamics directly to the width of the activation curve and peak sodium conductance. Figure 3 illustrates this relationship. An experimentally obtained activation curve from patches of cortical neurons<sup>13,14</sup> results in a shallow action potential onset (Fig. 3a, b). Increasing the steepness of the activation curve leads to sharper action potential onsets, but even with a fivefold increase, the simulated action potentials do not rise as fast as those recorded. Changing the effective peak sodium conductance—mimicking inactivation<sup>6,9</sup>—leaves the steepness of action potential onset unaffected but shifts the onset potentials (Fig. 3c, d). At the same time, increasing the steepness of the activation curve considerably decreases onset potential variability (Fig. 3e–f). Quantitatively, the variability of onset potentials is restricted by  $\Delta V \approx k \log G$ , where  $k$  is the width of the activation curve and  $G$  is the ratio of maximum to minimum peak conductance (see Supplementary Information). To mimic the measured combinations of onset rapidness and variability, unphysiologically large values of  $G$  (about 20,000) would be required.

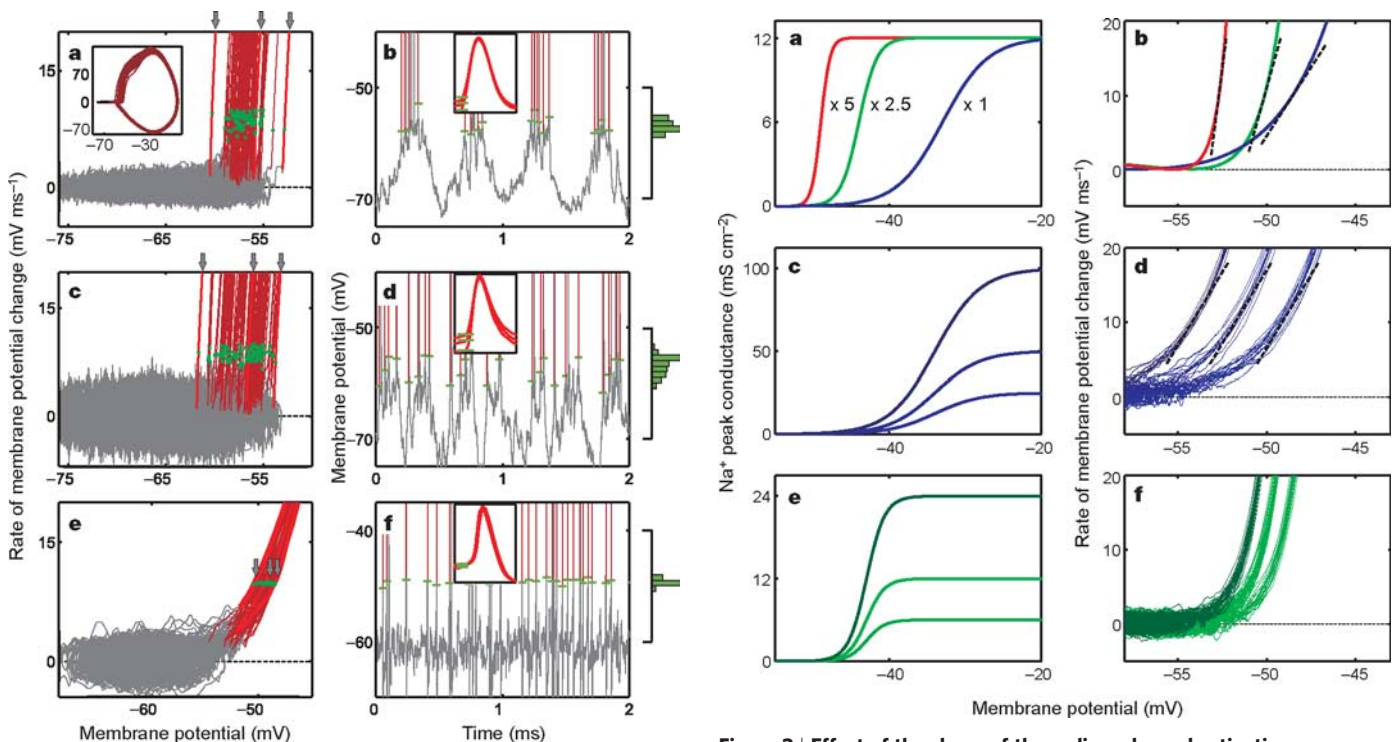


**Figure 2 | Different action potential initiation in visual cortex neurons recorded *in vivo* and in a Hodgkin–Huxley-type model subject to fluctuating synaptic inputs.** **a**, Phase plot of a simple cell response to a moving grating of optimal orientation. Subthreshold fluctuations are shown in grey, action potentials in red, and green dots indicate action potential onsets. The inset shows the complete trace. Arrows indicate three sample action potentials. **b**, Part of the recording from **a**, using the same colour code, with action potentials truncated in amplitude. Green bars show action potential onset potentials. Inset shows the action potentials marked with arrows in **a**. The histogram to the right shows the distribution of action potential onset potentials. **c**, **d**, Response of a complex cell. **e**, **f**, Response of a Hodgkin–Huxley-type model<sup>5</sup> subject to fluctuating synaptic input.

**Figure 3 | Effect of the shape of the sodium channel activation curve and effective peak conductance on action potential initiation in a Hodgkin–Huxley-type model.** Activation curves used in the model (**a**, **c**, **e**) and initial phases of resulting action potentials (**b**, **d**, **f**) are shown using matched colours. Blue lines show standard activation curves<sup>14</sup>. **a**, **b**, Increasing the steepness of the activation curve (**a**) leads to a more rapid action potential upstroke (**b**). Dashed lines indicate tangents at  $10 \text{ mV ms}^{-1}$ . **c**–**f**, Initiation of action potentials with shallow (**c**, **d**) and steep (**e**, **f**) activation curves and different sodium peak conductances in a model driven by fluctuating synaptic inputs (several action potentials superimposed). Changing peak conductance shifts the action potential onset potential but does not affect its onset rapidness. Steeper activation curves lead to smaller action potential onset spans (**d**, 6 mV; **f**, 2.5 mV).

To quantitatively compare the action potential onset dynamics in our recordings with action potential dynamics in Hodgkin–Huxley-type models, we plotted the action potential onset span (difference between maximum and minimum onset potential in a recording) against the rapidness of action potential onset (the slope of the phase plot at  $dV/dt = 10 \text{ mV ms}^{-1}$ ) for real and simulated recordings (Fig. 4). In the simulations, we used two different models<sup>5,10</sup> driven by fluctuating synaptic currents. In both models we systematically changed the peak sodium conductance and the activation curve over the entire range in which action potentials were generated. The locations of data points from the model simulations reflect the antagonism between onset span and rapidness. Simulated action potentials either showed a large onset rapidness or a large onset span, but never both. The points representing simulated action potentials are clearly separated from the points representing *in vivo* action potentials, which show rapid onset dynamics and large variability in onset potentials, irrespective of the electrophysiological cell type. Action potentials recorded *in vitro* had similarly fast onset dynamics (Fig. 4).

The above arguments and our extensive simulations indicate that the dynamics of action potential initiation in cortical neurons deviates qualitatively from the classical picture described by the Hodgkin–Huxley framework. What could be the biophysical mechanism that enables cortical action potentials to initiate much faster and at the same time with a much larger onset potential variability than predicted by the Hodgkin–Huxley theory? According to this theory, there is a one-to-one relationship between the single-channel activation curve and the action potential onset dynamics, owing to the assumption that the opening of individual sodium channels is statistically independent. This assumption, however, might be violated in the highly organized molecular machinery of a living

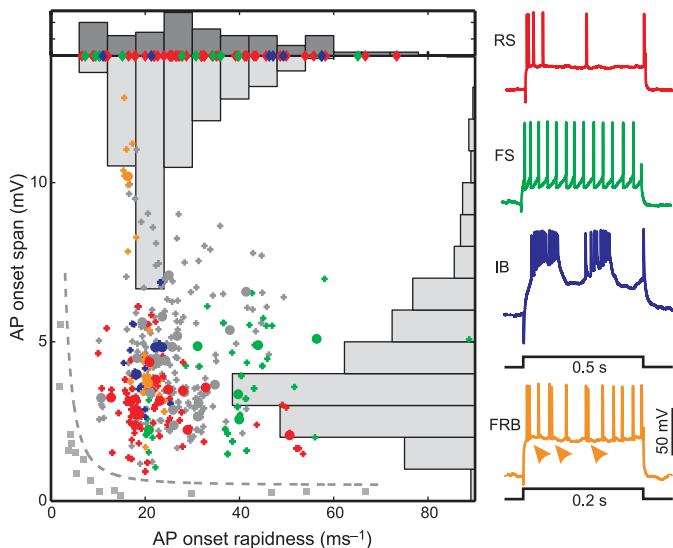


**Figure 4 | Action potential onset span and rapidness in cortical neurons and Hodgkin–Huxley-type models.** Points show data from cat visual cortex neurons *in vivo*, classified electrophysiologically as regular spiking (RS), fast spiking (FS), intrinsically bursting (IB) or fast rhythmic bursting (FRB). Colours match the neuronal responses to current steps shown on the right. Grey points indicate electrophysiologically unidentified cells. Circles show the mean of several measurements for each cell (individual measurements indicated with crosses). Diamonds at the top of the panel show *in vitro* data (cat visual cortex in blue, rat visual cortex in red, mouse hippocampus in green). Grey squares show simulation results from two Hodgkin–Huxley-type models with varied sodium channel activation curves and peak conductances, driven by fluctuating synaptic inputs. Dashed grey line separates the model from experimentally derived data. Histograms show the marginal distributions of the *in vivo* (light grey bars) and *in vitro* (dark grey bars) data.

cell. Indeed, the rapid onset of action potentials suggests that many sodium channels open virtually simultaneously, that is, in a potentially cooperative fashion.

To assess whether cooperative activation of voltage-gated sodium channels can account for the two characteristic features of cortical action potential initiation, we constructed a model of a population of coupled sodium channels. In this model, the gating of individual sodium channels follows a scheme introduced by Aldrich, Corey, and Stevens<sup>15</sup>. It incorporates state-dependent inactivation from the open state and voltage-dependent inactivation from closed states<sup>15,16</sup>. The key feature of our model is a coupling between neighbouring channels: the opening of a channel shifts the activation curve of each channel to which it is coupled towards more hyperpolarized values, thus increasing its probability of opening.

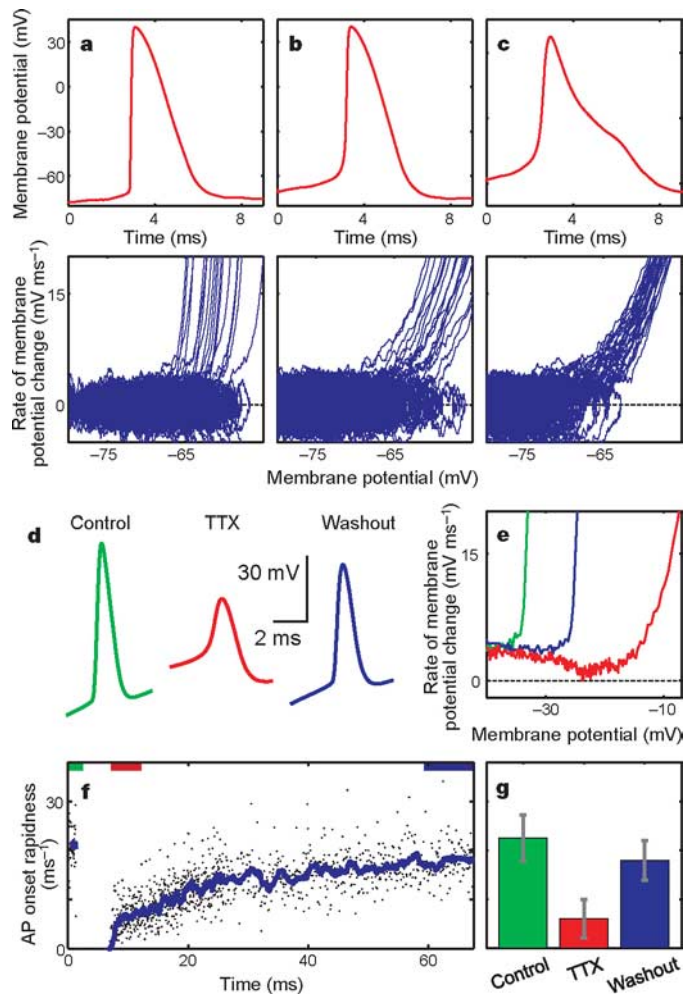


**Figure 5 | Cooperative activation of voltage-gated sodium channels can account for the dynamics of action potential initiation in cortical neurons.** **a**, Waveform (top) and phase plot (bottom) of action potentials elicited by fluctuating inputs in a conductance-based model that incorporates cooperative activation of sodium channels and closed-state inactivation. Both the action potential onset potential variability and onset rapidness are comparable to the *in vivo* recordings in Fig. 2. **b**, **c**, Same model, but without inter-channel coupling (**b**), and with Hodgkin–Huxley-like channel activation (**c**). **d–g**, Reducing the effective density of available sodium channels through TTX application reversibly reduces action potential amplitude and onset rapidness in cortical neurons *in vitro*. Shown are action potential waveforms (**d**) and phase plots of their initial parts (**e**). **f**, Time course of action potential onset rapidness in a cortical neuron before, during and after TTX application. **g**, Reversible reduction in onset rapidness of action potentials by TTX in six neurons. Error bars indicate s.e.m.

This model is able to reproduce the key features of cortical action potential initiation (Fig. 5a–c). With strongly cooperative activation, voltage-dependent inactivation from closed states, and slow de-inactivation (recovery from inactivation) of sodium channels, the simulated action potentials show both a large onset rapidness and large variability in onset potentials (Fig. 5a). Turning off the inter-channel coupling made the onset dynamics much shallower, while leaving onset variability unaffected (Fig. 5b). Hodgkin–Huxley-type dynamics of action potential onset was recovered when inactivation and de-inactivation were set to be fast and voltage-independent (Fig. 5c).

Assuming that channel interactions are distance-dependent in neuronal membranes, our model predicts that reducing the effective density of channels should weaken cooperativity, reduce the action potential onset rapidness and eventually lead to Hodgkin–Huxley-type onset dynamics. We tested this prediction *in vitro*, recording action potentials while reducing the density of available sodium channels by the application of tetrodotoxin (TTX). As expected, TTX application led to a decrease in action potential amplitude (Fig. 5d). More importantly, it also led to a substantial reduction in the onset rapidness of action potentials (Fig. 5d, e) in all tested cortical neurons (Fig. 5g), as predicted by our model. Moreover, gradual recovery of the number of available sodium channels during washout of TTX led to a gradual increase in action potential onset rapidness (Fig. 5f). These results cannot be explained by Hodgkin–Huxley-type models, in which reduction in the sodium channel density modifies only the amplitude of action potentials and their onset potential, but not their onset rapidness (see Fig. 3). Thus, in our opinion the fact that the dynamics of action potential initiation deviates qualitatively from voltage-dependent single channel activation points towards the cooperative activation of voltage-gated sodium channels.

Although our results are unexpected from a biophysical perspective, the combination of rapid dynamics and variable onset potentials of action potentials is beneficial for the coding of fast signals<sup>3,4</sup> (see also Supplementary Information). With Hodgkin–Huxley-type dynamics of action potential initiation, the encoding of signals that vary on a timescale of less than 10 ms requires unphysiologically high mean firing rates that are likely to be energetically prohibitive<sup>17,18</sup>. With action potential onset dynamics as described here for cortical neurons, much lower mean firing rates can support the encoding of such rapidly varying signals.

## METHODS

**In vivo and in vitro experiments.** *In vivo* intracellular recordings were made using sharp electrodes in adult cats (3.0–4.5 kg). Data from 47 cells were used for the analysis. In each cell, we recorded responses to the presentation of moving gratings of different orientations (duration 5–7 s), and periods of spontaneous activity (10–120 s). Cells were classified functionally as either simple or complex using the spike response modulation index, and electrophysiologically by their responses to depolarizing current steps. *In vitro*, whole-cell recordings were made with patch electrodes in slices of rat or cat visual cortex and rat or mouse hippocampus. Data from 17 rat, 3 mouse and 2 cat neurons were analysed.

**Computational models.** We used two conductance-based Hodgkin–Huxley-type models<sup>5,10</sup>, constructed to match the subthreshold membrane potential dynamics and firing statistics of cortical neurons. We introduced modifications to the models and varied model parameters over wide ranges in an attempt to reproduce the experimentally observed dynamics of action potential initiation. Action potential initiation by cooperative sodium channel activation was modelled using an effective mean field dynamics for a population of interacting sodium channels.

Details of experimental procedures and data analysis, and definitions of the models, their modifications and parameter ranges are provided in the Supplementary Information.

Received 22 October 2005; accepted 27 January 2006.

- Bernstein, J. Ueber den zeitlichen Verlauf der negativen Schwankung des Nervenstroms. *Pflügers Arch.* **1**, 173–207 (1868).
- Huxley, A. F. *Nobel Lectures, Physiology or Medicine 1963–1970* (Elsevier, Amsterdam, 1972).
- Fourcaud-Trocmé, N., Hansel, D., van Vreeswijk, C. & Brunel, N. How spike generation mechanisms determine the neuronal response to fluctuating inputs. *J. Neurosci.* **23**, 11628–11640 (2003).
- Naundorf, B., Geisel, T. & Wolf, F. Action potential onset dynamics and the response speed of neuronal populations. *J. Comput. Neurosci.* **18**, 297–309 (2005).
- Destexhe, A. & Paré, D. Impact of network activity on the integrative properties of neocortical pyramidal neurons *in vivo*. *J. Neurophysiol.* **81**, 1531–1547 (1999).
- Azouz, R. & Gray, C. M. Dynamic spike threshold reveals a mechanism for synaptic coincidence detection in cortical neurons *in vivo*. *Proc. Natl Acad. Sci. USA* **97**, 8110–8115 (2000).
- Volgushev, M., Pernberg, J. & Eysel, U. T. A novel mechanism of response selectivity of neurons in cat visual cortex. *J. Physiol. (Lond.)* **540**, 307–320 (2002).
- Azouz, R. & Gray, C. M. Adaptive coincidence detection and dynamic gain control in visual cortical neurons *in vivo*. *Neuron* **37**, 513–532 (2003).
- Henze, D. A. & Buzsáki, G. Action potential threshold of hippocampal pyramidal cells *in vivo* is increased by recent spiking activity. *Neuroscience* **105**, 121–130 (2001).
- Wang, X. J., Liu, Y., Sanchez-Vives, M. V. & McCormick, D. A. Adaptation and temporal decorrelation by single neurons in the primary visual cortex. *J. Neurophysiol.* **89**, 3279–3293 (2003).
- Schneidman, E., Freedman, B. & Segev, I. Ion channel stochasticity may be critical in determining the reliability and precision of spike timing. *Neural Comput.* **10**, 1679–1703 (1998).
- Patlak, J. Molecular kinetics of voltage-dependent Na<sup>+</sup> channels. *Physiol. Rev.* **71**, 1047–1080 (1991).
- Huguenard, J. R., Hamill, O. P. & Prince, D. A. Developmental changes in Na<sup>+</sup> conductances in rat neocortical neurons: appearance of a slowly inactivating component. *J. Neurophysiol.* **59**, 778–795 (1988).
- Colbert, C. M. & Pan, E. Ion channel properties underlying axonal action potential initiation in pyramidal neurons. *Nature Neurosci.* **5**, 533–538 (2002).
- Aldrich, R. W., Corey, D. P. & Stevens, C. F. A reinterpretation of mammalian sodium channel gating based on single channel recording. *Nature* **306**, 436–441 (1983).
- Goldman, L. Stationarity of sodium channel gating kinetics in excised patches from neuroblastoma N1E 115. *Biophys. J.* **69**, 2364–2368 (1995).
- Attwell, D. & Laughlin, S. B. An energy budget for signaling in the grey matter of the brain. *J. Cereb. Blood Flow Metab.* **21**, 1133–1145 (2001).
- Lennie, P. The cost of cortical computation. *Curr. Biol.* **13**, 493–497 (2003).

Supplementary Information is linked to the online version of the paper at [www.nature.com/nature](http://www.nature.com/nature).

**Acknowledgements** We would like to thank A. Borst, M. Brecht, M. Chistiakova, T. Geisel, T. Kottos, T. Moser, E. Neher, W. Stühmer, I. Timofeev and C. van Vreeswijk for discussions, A. Borst, M. Brecht and E. Neher for comments on earlier versions of the manuscript, and A. Malyshev for help in some of the experiments. This study was supported by grants from the Deutsche Forschungsgemeinschaft to M.V., by grants from the Human Frontier Science Program and the Bundesministerium für Bildung und Forschung to F.W., and by the Max-Planck Society.

**Author Contributions** B.N., F.W. and M.V. contributed equally to this work. All authors discussed the results and commented on the manuscript.

**Author Information** Reprints and permissions information is available at [npg.nature.com/reprintsandpermissions](http://npg.nature.com/reprintsandpermissions). The authors declare no competing financial interests. Correspondence and requests for materials should be addressed to F.W. ([fred@chaos.gwdg.de](mailto:fred@chaos.gwdg.de)).

## NEUROPHYSIOLOGY

## Hodgkin and Huxley model — still standing?

Arising from: B. Naundorf, F. Wolf & M. Volgushev *Nature* 440, 1060–1063 (2006)

Action potentials in cortical neurons show a variable threshold and a sudden rise in membrane potential at initiation. Naundorf *et al.*<sup>1</sup> fail to explain these features using single- or double-compartment Hodgkin–Huxley-style models, suggesting instead that they could arise from cooperative opening of Na<sup>+</sup> channels, although there is no direct biological evidence to support this. Here we show that these so-called unique features are to be expected from Hodgkin–Huxley models if the spatial geometry and spike initiation properties of cortical neurons are taken into account — it is therefore unnecessary to invoke exotic channel-gating properties as an explanation.

Cortical pyramidal cells initiate spikes in the axon initial segment (AIS) about 30–60 μm from their soma. These spikes then propagate antidromically through the soma and dendrites<sup>2–4</sup>. A well known feature of antidromic spikes is their sudden rise from baseline<sup>5</sup>. These critical properties were not considered by Naundorf *et al.*<sup>1</sup>.

We made simultaneous whole-cell recordings from the AIS by patching the cut end of the axon (Fig. 1, legend) and the soma of layer-5 pyramidal neurons *in vitro*<sup>6</sup> during spontaneous spike generation (Fig. 1). Somatic spikes showed a rapid rise, or 'kink', at initiation (Fig. 1a, b) and the slope of the phase plot of spike dV/dt versus V at dV/dt = 15 mV ms<sup>-1</sup> was 25 ± 6.8 ms<sup>-1</sup> (mean ± s.d.; n = 32). The phase plots of dV/dt versus V typically revealed a biphasic rise, which was suggestive of two underlying components (Fig. 1b, c), as observed in many cell types<sup>7,8</sup>. This biphasic component was not evident in the recordings of Naundorf *et al.*<sup>1</sup>, although the low peak dV/dt of their recordings indicates that their spikes may not have been fully represented.

Intracellular injection of a noisy conductance that mimics the arrival of excitatory and inhibitory synaptic activity<sup>9</sup> resulted in significant variation in the apparent spike threshold (n = 6; Fig. 1c, green lines), as observed in the recordings of Naundorf *et al.*<sup>1</sup>.

In contrast to somatic spikes, those recorded at the site of spike initiation, the AIS, showed a slower rise (n = 10; Fig. 1d, e). The slope of the phase plot of spike dV/dt versus V at dV/dt = 15 mV ms<sup>-1</sup> was much lower for the AIS (3.8 ± 1.7 ms<sup>-1</sup>; n = 6; P < 0.01; Fig. 1d, e) than it was for the soma (Fig. 1a, b). The slow rise at spike initiation in the AIS is not an artefact of our method of axonal recording (Fig. 1, legend). On intracellular injection of a noisy conductance that mimics synaptic activity<sup>9</sup>, the apparent

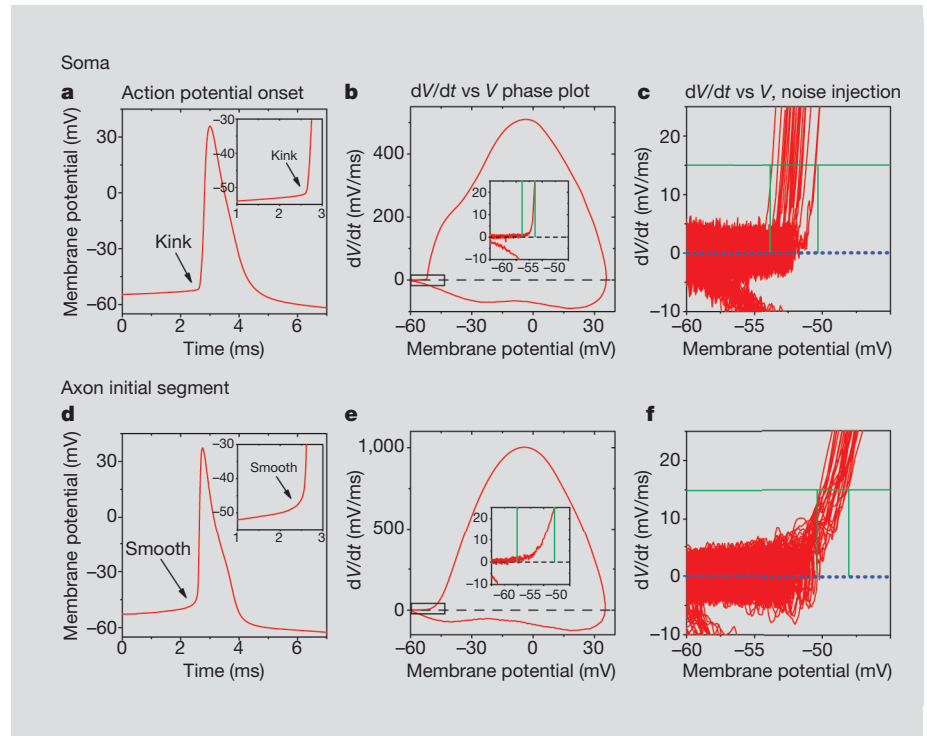


**Figure 1 | Properties of spike initiation in the soma and axon of cortical pyramidal cells.** **a**, Somatic spike exhibits a 'kink' at its onset. **b**, Phase plot (dV/dt versus V) and close-up of rapid initiation (inset) of the spike shown in **a**. **c**, Close-up of the phase plot of somatic spike initiation during noisy intrasomatic current injection<sup>9</sup>, showing a broad distribution of thresholds (green lines). **d**, Whole-cell axonal recording (50 μm from the soma). **e**, Phase plot of the axonal spike. Note the smoothly rising dV/dt. **f**, Overlay of dV/dt versus V for the onset of axonal spikes, showing lower variability (compare with the soma) of spike threshold (green lines).

**Methods.** Simultaneous axonal and somatic whole-cell recordings were obtained with the multiclamp 700B amplifier from ferret prefrontal cortical layer-5 pyramidal cells in slices maintained *in vitro* at 36 °C (ref. 6). Spikes shown in **a**, **d**, as well as in **c**, **f**, were recorded simultaneously. Spikes occurred either during spontaneous synaptic activity<sup>6</sup> or in response to the intrasomatic injection of a noisy (10–15 mV) current injection<sup>9</sup>. Whole-cell axonal recordings obtained through patching the cut end of the axon (terminal bleb) do not result in abnormal smoothness of spikes because spikes recorded from distal (> 100 μm) axonal sites also show an onset kink owing to spike propagation (see also www.mccormicklab.org).

spike threshold was less variable for the AIS (n = 6; Fig. 1f, green lines) than it was for the soma (Fig. 1c).

Spike initiation in the AIS is mediated by either a high Na<sup>+</sup>-channel density in the AIS, as indicated by immunocytochemistry<sup>10,11</sup>, or by a lesser density of Na<sup>+</sup> channels, which have a low threshold for activation<sup>12</sup>. Using a previous model of spike initiation in a layer-5 cortical pyramidal cell<sup>13</sup>, we adjusted the axonal and somatic densities of Na<sup>+</sup> and K<sup>+</sup> channels until the spike waveform and its derivative were similar to those of our actual recordings (compare Figs 1 and 2).

Our Hodgkin–Huxley model initiated spikes in the AIS that then propagated antidromically through the soma and dendrites, as

in real pyramidal cells. At the soma, these spikes showed a rapid rise at initiation (Fig. 2a, b), and the slope of the phase plot for spike initiation at dV/dt = 15 mV ms<sup>-1</sup> was 21 ms<sup>-1</sup>. Intracellular injection of artificial synaptic barrages<sup>9</sup> into the modelled neuron revealed a high variability of apparent spike threshold in the soma (Fig. 2c).

As in the whole-cell recordings, the rise in the model spike at initiation was smoother at the AIS (Fig. 2d, e) than at the soma (Fig. 2a, b). The slope of the phase plot for spike initiation at dV/dt = 15 mV ms<sup>-1</sup> was considerably lower for the model AIS (4 ms<sup>-1</sup>) than for the soma, and both were in the range observed in normal cells. Intracellular injection of artificial synaptic barrages<sup>9</sup> showed a less variable threshold in

the AIS (Fig. 2f) than in the soma (Fig. 2c), as we found for real neurons (Fig. 1c, f).

We found that several other Hodgkin–Huxley models of cortical pyramidal cells, even one based on a relatively low density of Na<sup>+</sup> conductance in the axon, replicated the ‘kink’ and variability of somatic spikes (Fig. 2 legend). These features of spike initiation in the soma were dependent on the initiation of spikes in the AIS: increasing the somatic Na<sup>+</sup> conductance to a high level (7.5 nS μm<sup>-2</sup>) and removing Na<sup>+</sup> conductance from the axon in the model presented here resulted in a loss of the kink at the foot of the spike (soma slope, 4.1 ms<sup>-1</sup>) and a reduction in spike threshold variability in the soma (results not shown).

Our findings reveal that leading Hodgkin–Huxley models of cortical pyramidal cell spike initiation capture the so-called unique features observed by Naundorf *et al.*<sup>1</sup> We attribute these features simply to recording from a site that is distant from the site of spike initiation and to the non-uniform distribution of spike properties over the somatic and axonal membrane. The initiation of spikes in the axon that then back-propagate into the soma can result in a rapid change in membrane potential (the kink) at the foot of the somatic spike. The large current supplied by the axonal spike precedes and overlaps with the current supplied by the local generation of the action potential in the soma during the rising phase of the spike. This results in a more rapid rise at the foot of the spike in the soma than would occur if there were no preceding spike in the axon. The apparent high threshold variability with intrasomatic recordings merely results from membrane potential differences between the soma and the actual site of spike initiation, the axon, at the time that spikes are generated. These membrane-potential differences arise from local electrophysiological differences, as well as spatial non-uniformity in synaptic activity. We conclude that the observations made by Naundorf *et al.*<sup>1</sup> are predictable by Hodgkin–Huxley theory and the known physiology of spike initiation<sup>2–4</sup>, and that there is no need to invoke exotic interchannel cooperativity to explain their observations.

David A. McCormick\*, Yousheng Shu\*†, Yuguo Yu\*

\*Department of Neurobiology, Kavli Institute for Neuroscience, Yale University School of Medicine, New Haven, Connecticut 06510, USA  
e-mail: david.mccormick@yale.edu

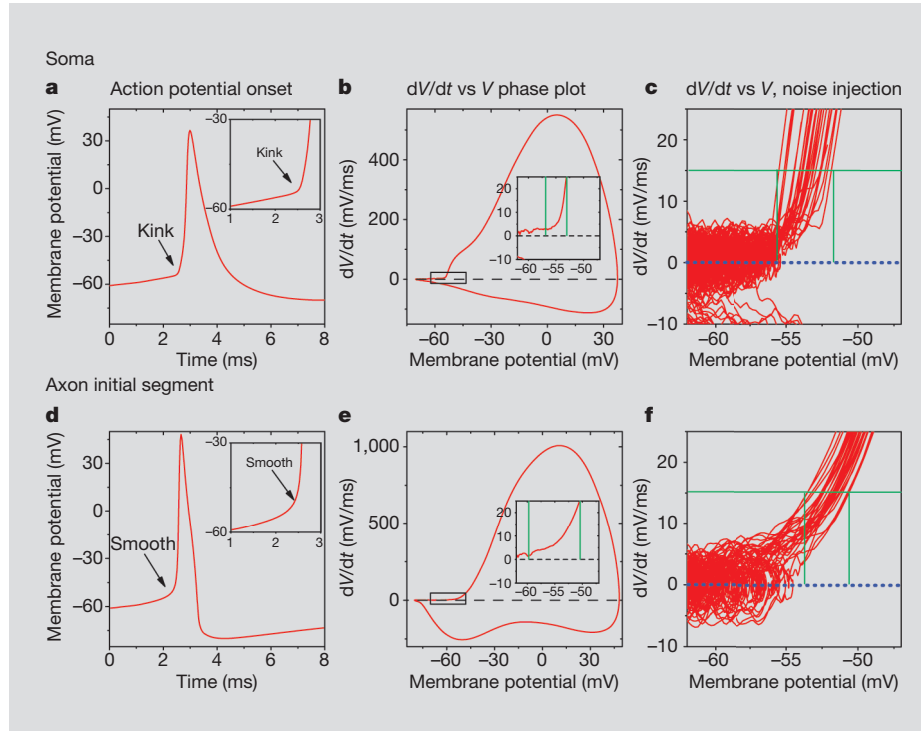


**Figure 2 | Hodgkin–Huxley model of a layer-5 cortical pyramidal cell.** **a**, Somatic spike shows a ‘kink’ at its onset, as in the real neuron. **b**, Phase plot ( $dV/dt$  versus  $V$ ) and close-up of rapid initiation (inset) of the spike shown in **a**. **c**, Close-up of the phase plot of somatic spike during noisy intrasomatic current injection, showing a broad distribution of thresholds (green lines). **d**, Axonal spike (45 μm from the soma). **e**, Phase plot of the axonal spike. Note the smoothly rising  $dV/dt$ . **f**, Overlay of  $dV/dt$  versus  $V$  for the onset of axonal spikes, showing lower variability of spike threshold (green lines).

**Methods.** Results were obtained from a model layer-5 cortical pyramidal cell<sup>15</sup> with the intrasomatic injection of a 10–15 mV noisy conductance. The model contained the following conductances: soma (Na<sup>+</sup>, 0.75 nS μm<sup>-2</sup>; K<sup>+</sup>, 0.15 nS μm<sup>-2</sup>); axon hillock and initial segment (Na<sup>+</sup>, 7.5 nS μm<sup>-2</sup>; K<sup>+</sup>, 1.5 nS μm<sup>-2</sup>); dendrite (Na<sup>+</sup>, 0.1 nS μm<sup>-2</sup>; K<sup>+</sup>, 0.002 nS μm<sup>-2</sup>; M-current, 0.0003 nS μm<sup>-2</sup>). Axonal length, 50 μm; soma size, 20 × 30 μm. These parameters were used to match the maximal  $dV/dt$  rates, durations and initiation site of spikes in our neurons (Fig. 1). Similar results are obtained from several Hodgkin–Huxley models of cortical pyramidal cells, including those using a high, medium or relatively low density of axonal Na<sup>+</sup> conductance<sup>12–14</sup>, and the results from these simulations were well within the range of real cortical cells (see also [www.mccormicklab.org](http://www.mccormicklab.org)).

†Present address: Institute of Neuroscience, Chinese Academy of Science, Shanghai 200031, China

- Naundorf, B., Wolf, F. & Volgushev, M. *Nature* **440**, 1060–1063 (2006).
- Palmer, L. M. & Stuart, G. J. *J. Neurosci.* **26**, 1854–1863 (2006).
- Stuart, G., Schiller, J. & Sakmann, B. *J. Physiol.* **505**, 617–632 (1997).
- Shu, Y., Duque, A., Yu, Y., Haider, B. & McCormick, D. A. *J. Neurophysiol.* doi:10.1152/jn.00922.2006 (2006).
- Pare, D., Shink, E., Gaudreau, H., Destexhe, A. & Lang, E. J. *J. Neurophysiol.* **79**, 1450–1460 (1998).
- Shu, Y., Hasenstaub, A., Duque, A., Yu, Y. & McCormick, D. A. *Nature* **441**, 761–765 (2006).

- Colbert, C. M. & Johnston, D. *J. Neurosci.* **16**, 6676–6686 (1996).
- Coombs, J. S., Curtis, D. R. & Eccles, J. C. *J. Physiol.* **139**, 232–249 (1957).
- Shu, Y., Hasenstaub, A., Badoual, M., Bal, T. & McCormick, D. A. *J. Neurosci.* **23**, 10388–10401 (2003).
- Inda, M. C., DeFelipe, J. & Munoz, A. *Proc. Natl Acad. Sci. USA* **103**, 2920–2925 (2006).
- Komada, M. & Soriano, P. *J. Cell Biol.* **156**, 337–348 (2002).
- Colbert, C. M. & Pan, E. *Nature Neurosci.* **5**, 533–538 (2002).
- Mainen, Z. F. & Sejnowski, T. J. *Nature* **382**, 363–366 (1996).
- Baranauskas, G. & Martina, M. *J. Neurosci.* **26**, 671–684 (2006).

doi:10.1038/nature05523

## NEUROPHYSIOLOGY

# Naundorf *et al.* reply

Replying to: D. A. McCormick, Y. Shu & Y. Yu *Nature* **445**, 10.1038/nature05523 (2007)

McCormick *et al.*<sup>1</sup> question whether the rapid onset and highly variable thresholds of action potentials<sup>2</sup> are genuine features of cortical action-potential generators — that is,

whether they reflect the voltage-dependence of the underlying sodium currents. Instead, they consider these features to be epiphenomena, reflecting lateral currents from a

remote initiation site, and, contrary to direct evidence<sup>3</sup>, they assume that sodium currents show canonical kinetics.

Although the lateral current hypothesis of